LETTER

Modified theory of a microperforated panel with roughened perforations

To cite this article: Zhimin Xu *et al* 2019 *EPL* **125** 34004

A Letters Journal Exploring the Frontiers of Physics

February 2019

EPL, **125** (2019) 34004 www.epljournal.org
doi: 10.1209/0295-5075/125/34004

Modified theory of a microperforated panel with roughened perforations

Zhimin Xu[1,2], Xiangjun Peng[1,2], Xuewei Liu[1,2], Fengxian Xin[1,2(a)] and Tian Jian Lu[3(b)]

[1] *State Key Laboratory for Strength and Vibration of Mechanical Structures, Xi'an Jiaotong University Xi'an 710049, PRC*
[2] *MOE Key Laboratory for Multifunctional Materials and Structures, Xi'an Jiaotong University - Xi'an 710049, PRC*
[3] *State Key Laboratory of Mechanics and Control of Mechanical Structures, Nanjing University of Aeronautics and Astronautics - Nanjing 210016, PRC*

received 16 September 2018; accepted in final form 4 February 2019
published online 11 March 2019

PACS 43.20.+g – General linear acoustics
PACS 43.55.Ev – Sound absorption properties of materials: theory and measurement of sound absorption coefficients; acoustic impedance and admittance

Abstract – Microperforated panels (MPPs) play important roles in sound absorbing systems. The classical Maa theory for the MPPs is modified to account for the effect of roughness on the surface of microperforations on sound absorption. Correspondingly, the relative acoustic resistance and relative acoustic mass of the system are determined theoretically. Full numerical simulations with the method of finite elements are performed on the roughened MPP to validate the modified theory, with good agreement achieved. It is demonstrated that surface roughness decreases resonant frequency and promotes viscous dissipation, thus enhancing the sound absorbing capability of the MPP. This work extendes Maa's theory for the sound absorption of MPP from smooth perforations to rough perforations. The modified theory for MPP with roughened perforations has a great significance in sound absorption field, since it is more applicable for the realistic situations.

Noise control has become a pressing issue in modern society. To solve the problem, numerous sound absorbing materials and structures, such as open-cell cellular foams, porous structures and fibrous rock wool [1], have been developed and widely used in architectural design, transportation, mechanical engineering, and other fields. One typical problem associated with the commonly applied sound absorbing materials/structures is the difficulty in adjusting the sound absorbing effect. Traditional methods [2,3] (for porous materials) including changing the material thickness, changing the pore size and porosity are not satisfactory for they are not flexible enough to manipulate. To address the issue, Maa [4,5] put forward the inspiring concept of microperforated panel (MPP) and developed a theory to describe its acoustic performance.

The MPP structure is designed based on the classical Helmholtz resonator. Typically, it is composed of two parts: a thin panel having periodically arranged circular microperforations (usually of sub-millimeter scale) and an air gap backed to the panel. The air gap can be considered as a resonant cavity, while the microperforations (microchannels) can be considered as mass blocks when the MPP is active. In the presence of a propagating sound wave, the channel surface generates viscous force and dissipates sound energy. The whole system thence becomes a spring-mass system with viscosity. The resonant frequency is determined by the volume of the air gap and the thickness of the channel, while the resonant peak is determined by the viscous force. The MPP not only exhibits good sound absorption performance, especially at relatively low frequencies, but also is fiber free, succinct, and robust to complex environment [6].

Although the Maa theory describes faithfully the sound absorption effect of a MPP with smooth perforations (MPP-S), the perforation surface often exhibits roughened morphology due to limited processing accuracy. In such cases, when air inside the pore oscillates to dissipate the energy of sound, the roughened pore surface inevitably affects the sound absorption performance of the MPP. Prior work has been undertaken to reveal how a rough surface influences the flow properties [7,8]. Even when the

(a) E-mail: fengxian.xin@gmail.com (corresponding author)
(b) E-mail: tjlu@nuaa.edu.cn (corresponding author)

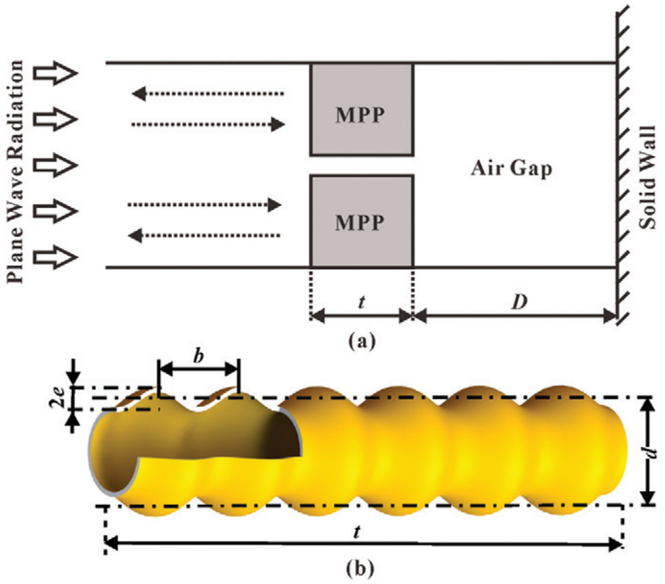

Fig. 1: (a) Microperforated panel (MPP) backed by air cavity as sound absorbing structure; (b) circular cylindrical pore with periodic axial surface roughness.

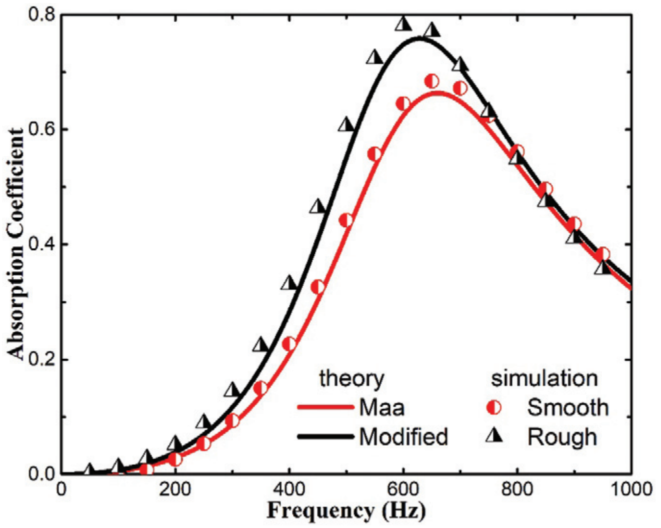

Fig. 2: Sound absorption coefficients of MPPs with rough pores and smooth pores: comparison between theoretical model predictions and FE simulation results, with $d = 1\,\mathrm{mm}$, $t = 6\,\mathrm{mm}$, $D = 50\,\mathrm{mm}$, $\phi = 0.0625$, $\varepsilon = 0.1$ and $\beta = 2\pi$.

surface roughness is small, it has been demonstrated [9] that the static flow resistivity is affected significantly by the roughness.

In the current study, we report how the absorption effect of a MPP with roughened perforations (MPP-R) can be different from that of the MPP-S by changing the parameters dictating the roughened structure. It is anticipated that surface roughness produces a larger absorption coefficient at low frequencies due to a larger acoustic mass. Built upon the Maa theory, a modified theory is developed to quantify the beneficial effect of surface roughness on sound absorption. Also, relevant acoustic properties of the MPP-R, such as relative acoustic mass and relative acoustic resistance, are calculated and compared with those of MPP-S. A parametric study is further performed to find out how the resonant frequency and maximum absorption coefficient change with varying roughness. The theoretical predictions are validated against numerical results obtained with direct finite element (FE) simulations.

The MPP sound absorbing system is composed of two parts, as shown in fig. 1(a), the MPP and the air gap, which assemble a Helmholtz resonator. When an acoustic wave is incident on the system, the air inside the MPP channel (pore) oscillates, thus inducing viscous energy dissipation. Let t denote the thickness of the panel, D the length of the air gap, d the average diameter of channel and ϕ the porosity of the MPP. With reference to fig. 1(b), the roughened boundary of the circular cylindrical pore is assumed to follow an idealized sinusoidal pattern, with amplitude e and wavelength b. Two dimensionless parameters are introduced to characterize the pore surface roughness: relative roughness $\varepsilon = e/d$ and wave number $\beta = 2\pi d/b$.

For traditional MPPs with smooth micro-pores, the sound absorption coefficient can be calculated by the Maa theory [4,5], as

$$\alpha = \frac{4r}{(1+r)^2 + (\omega m - \cot(\omega D/c))^2}, \qquad (1)$$

where c is the sound speed in air, ω is the angular frequency of incident acoustic wave, and r defined as the relative acoustic resistance, is given by

$$r = \frac{32\mu}{\rho\phi c}\frac{t}{d^2}\left[\sqrt{1+\frac{x^2}{32}} + \frac{\sqrt{2}x}{8}\frac{d}{t}\right], \qquad (2)$$

where ρ is air density and μ is the dynamic viscosity of air. In addition, m, defined as the relative acoustic mass, is

$$m = \frac{t}{\phi c}\left[1 + \frac{1}{\sqrt{9+\frac{x^2}{2}}} + 0.85\frac{d}{t}\right], \qquad (3)$$

where $x = \sqrt{\frac{\rho\omega}{\mu}}\frac{d}{2}$. Because the MPP sound absorbing system can be considered as a Helmholtz resonator, there exists an absorption peak (*i.e.*, maximum sound absorption coefficient)

$$\alpha_{\max} = \frac{4r}{(1+r)^2} \qquad (4)$$

at frequency ω_0 that is given by

$$m\omega_0 = \cot(\omega_0 D/c). \qquad (5)$$

For MPPs having roughened microperforations (fig. 1), the Maa theory as detailed above needs to be modified. To this end, existing analytical solutions of low Reynolds

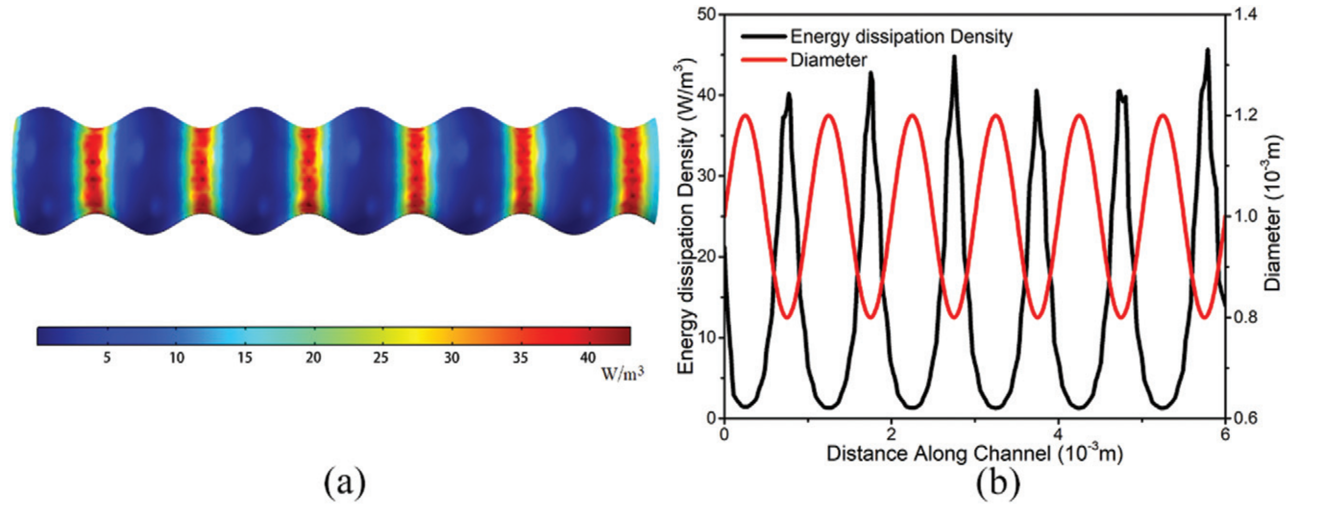

Fig. 3: Sound energy dissipation density in a rough channel: (a) cloud diagram; (b) curve graph, with $d = 1\,\text{mm}$, $t = 6\,\text{mm}$, $D = 50\,\text{mm}$, $\phi = 0.0625$, $\varepsilon = 0.1$ and $\beta = 2\pi$.

number flow of fluid inside a circular pipe with sinusoidal surface roughness are employed. According to our previous work [9], the static flow resistivity of the rough pipe is

$$(\sigma)_a = \frac{32\mu}{d^2}\left\{\left(\frac{(6\varepsilon^2+1)}{(1-4\varepsilon^2)^{3.5}} - \frac{1}{(1-2\varepsilon)^4}\right) \times \frac{2\mathrm{e}^{-\frac{1}{5\pi}\beta}}{1+\mathrm{e}^{-\frac{1}{5\pi}\beta}} + \frac{1}{(1-2\varepsilon)^4}\right\}. \quad (6)$$

Here, the factor $32\mu/d^2$ denotes the static flow resistivity of smooth pipes, and correspondingly, the tortuosity is

$$(\alpha_\infty)_a = 1 + \frac{\varepsilon^2\beta^2[(J_0^2(\beta/2) - J_1^2(\beta/2))]}{2J_1^2(\beta/2)}, \quad (7)$$

where ε and β are the relative roughness and wave number of the rough channel, respectively (fig. 1), and $J_k(\cdot)$ is the modified Bessel function of the first kind and k-th order. Once the relative resistance and relative mass of the roughened pipe (perforation) are determined, its specific acoustic impedance can be calculated using the model of Pride *et al.* [10] as

$$Z' = \left\{\frac{v}{j\omega q_0}\left\{\frac{1}{4}+\frac{3}{4}\left[1+\left(\frac{8\alpha_\infty q_0}{3\Lambda}\right)^2\frac{j\omega}{v}\right]^{1/2}\right\}+\alpha_\infty\right\}\rho\omega jt, \quad (8)$$

with the viscous characteristic length $\Lambda = \sqrt{8\mu\alpha_\infty/\sigma}$, the kinematic viscosity $\nu = \mu/\rho$, $j = \sqrt{-1}$ the imaginary unit, α_∞ the tortuosity and the viscous permeability $q_0 = \mu/\sigma$. Take the influence of end correction on the effective length of channel and acoustic resistance into consideration [4], it follows that the acoustic impedance is

$$z' = \frac{Z'}{\phi\rho c} + \frac{4\sqrt{2}\mu x}{\rho\phi c d} + \frac{0.85 d\omega j}{\phi c} = r' + j\omega m', \quad (9)$$

where (r', m') are the relative acoustic resistance and relative acoustic mass of the roughened perforation, respectively. Upon replacing (r,m) in eq. (1) by (r', m'), the sound absorption coefficient of the MPP-R system is determined.

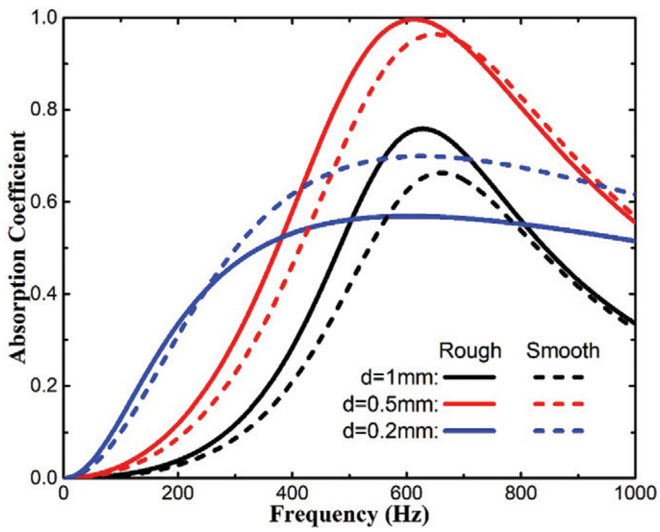

Fig. 4: Sound absorption of MPP-R and MPP-S with different diameters and with $t = 6\,\text{mm}$, $D = 50\,\text{mm}$, $\phi = 0.0625$, $\varepsilon = 0.1$ and $\beta = 2\pi$.

In order to validate the modified Maa model, full numerical simulations with the commercial FE code COMSOL are performed. Figure 2 compares the theoretical predictions and numerical results. Geometric parameters of the MPP-R system (fig. 1) examined are $d = 1\,\text{mm}$, $t = 6\,\text{mm}$, $D = 50\,\text{mm}$, $\phi = 0.0625$, $\varepsilon = 0.1$ and $\beta = 2\pi$. For comparison, the absorption coefficient of the corresponding MPP-S is also plotted in fig. 2 as a function of frequency. Overall, for both MPP-R and MPP-S systems, the theoretical predictions match well with the numerical results, and the presence of surface roughness on sound absorption is not negligible. Specifically, the resonant frequency of the MPP-R is about 50 Hz lower than the MPP-S, while the peak absorption coefficient of the former increases by

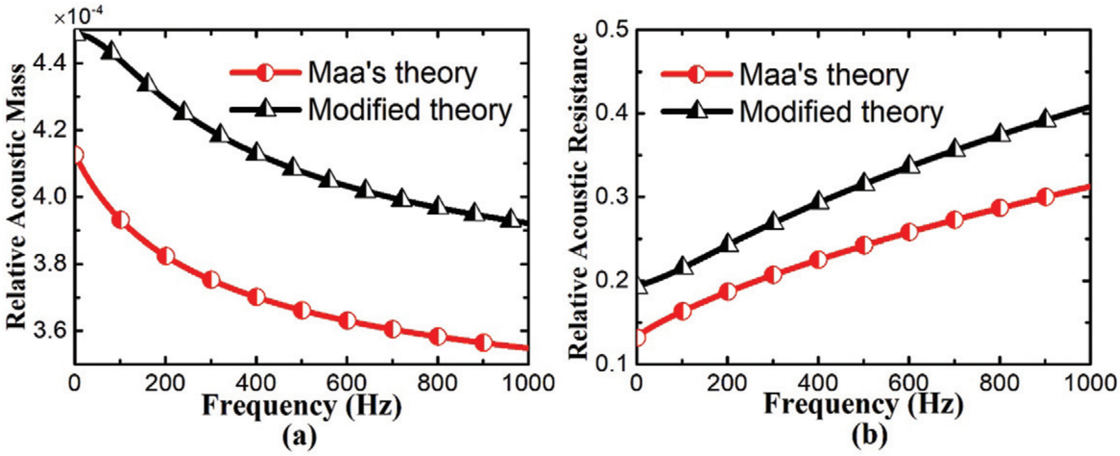

Fig. 5: Acoustic parameters of MPPs with rough pores and smooth pores ($d = 1\,\mathrm{mm}$, $t = 6\,\mathrm{mm}$, $D = 50\,\mathrm{mm}$, $\phi = 0.0625$, $\varepsilon = 0.1$, $\beta = 2\pi$): (a) acoustic mass; (b) acoustic resistance.

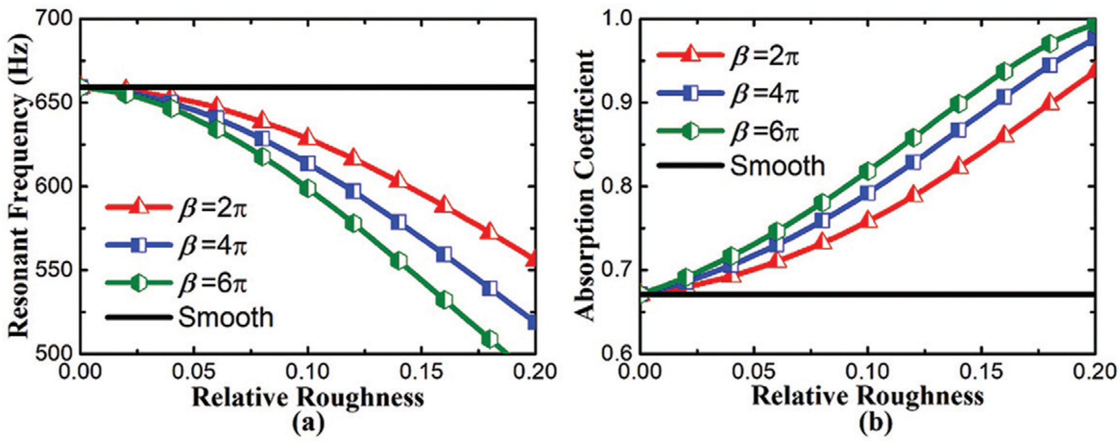

Fig. 6: Sound absorbing properties of MPP with rough pores and smooth pores ($d = 1\,\mathrm{mm}$, $t = 6\,\mathrm{mm}$, $D = 50\,\mathrm{mm}$, $\phi = 0.0625$): (a) resonant frequency; (b) peak absorption coefficient.

20%. These two features can be understood by comparing eqs. (2), (3) and (9).

To gain a fundamental understanding for the sound absorption mechanism, the sound energy dissipation in the rough perforation is explored in fig. 3. As shown in fig. 3, the sound energy dissipation density varies periodically along the channel length, due to the periodic change of the channel diameter. Specifically, the black line in fig. 3(b) depicts the energy dissipation density distribution and the red line plots the diameter variation along the channel length. The energy dissipation peak always locates at the position with minimum diameter, where the friction between air and wall is severe. In other words, when the sound wave propagates in the perforation channel, the friction between air and wall relates to the local diameter, by which it affects the viscous dissipation and heat transfer loss.

The results of fig. 3 demonstrate that the decrease of the channel diameter can enhance the friction and the energy dissipation of the perforation channel, however, it does not always mean that there is an improvement of the sound absorption performance of the channel. This is because the sound absorption performance relies on the entry energy of the sound wave and the dissipation ability (*i.e.*, the friction) of the channel. The combination of the two determines the real dissipated sound energy and the sound absorption performance. The decrease of the channel diameter will increase the dissipation ability but reduce the entry sound energy.

To clearly reveal the influence of the channel diameter, the sound absorption of the MPP-R and MPP-S with different diameters but same porosity is depicted in fig. 4. As shown in fig. 4, for the MPP-R and MPP-S, when the perforation diameter is reduced from $d = 1\,\mathrm{mm}$ to $d = 0.5\,\mathrm{mm}$, the sound absorption is significantly increased. This is because when reducing the perforation diameter from 1 mm to 0.5 mm, the entry sound energy is not reduced much, while the dissipation ability (*i.e.*, the friction) of the perforation channels is remarkably increased, the combination of the two effects leads to an enhanced sound absorption. However, when the perforation diameter is reduced from $d = 0.5\,\mathrm{mm}$ to $d = 0.2\,\mathrm{mm}$, the sound absorption is

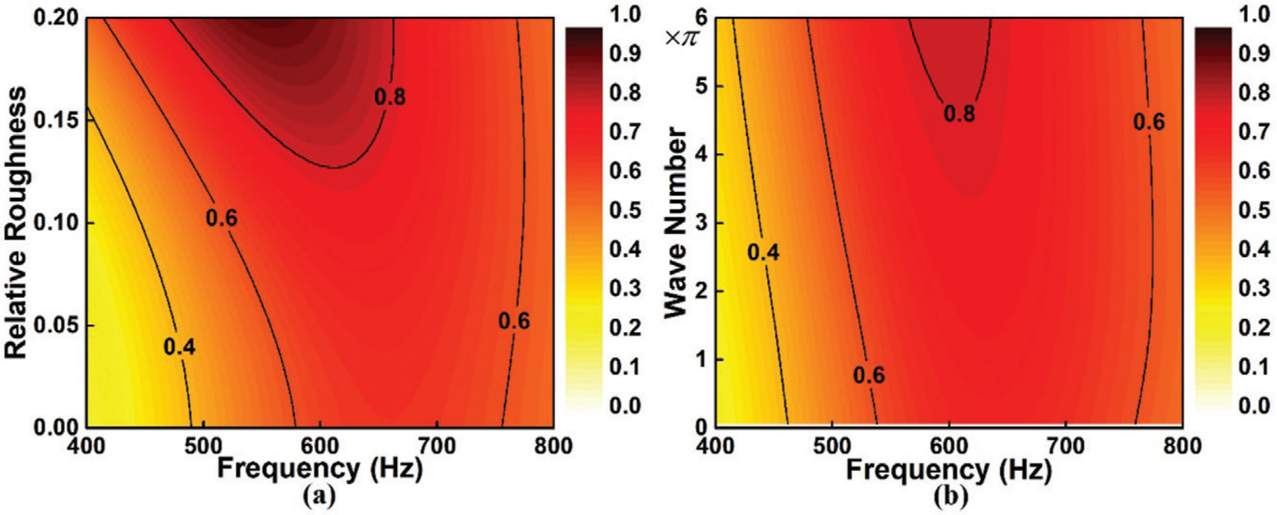

Fig. 7: Roughness effect on sound absorption coefficient ($d = 1\,\text{mm}$, $t = 6\,\text{mm}$, $D = 50\,\text{mm}$, $\phi = 0.0625$): (a) influence of relative roughness ($\beta = 2\pi$); (b) influence of wave number ($\varepsilon = 0.1$).

pronouncedly decreased. This is because when reducing the perforation diameter from 0.5 mm to 0.2 mm, most of the incident sound is reflected and only a small part can enter the perforation channels, although the dissipation ability (*i.e.*, the friction) of the perforation channels is remarkably increased, the combination of the two effects leads to a weakened sound absorption. Moreover, it is seen from fig. 4 that the sound absorption of MPP-R is larger than that of MPP-S for the $d = 1\,\text{mm}$ to $d = 0.5\,\text{mm}$ cases, but the sound absorption of MPP-R is smaller than that of MPP-S for the $d = 0.2\,\text{mm}$ case. For the $d = 1\,\text{mm}$ to $d = 0.5\,\text{mm}$ cases, the roughened wall increases the dissipation ability (*i.e.*, the friction) of the perforation channels but does not reduce the entry sound energy much, resulting in the sound absorption improvement of the MPP-R. For the $d = 0.2\,\text{mm}$ case, the roughened wall increases the dissipation ability of the perforation channels but reduces the entry sound energy much, resulting in the sound absorption reduction of the MPP-R. Also, it is noticed that the peak frequency of sound absorption remains the same, since the acoustic mass (because of the fixed porosity) and the cavity thickness remain unchanged.

Figure 5 makes a comparison of the predicted relative acoustic resistance and relative acoustic mass between MPP-R and MPP-S. In the presence of roughness, the relative acoustic mass increases by $\sim$10% in the whole frequency range considered (fig. 5(a)), whereas the relative acoustic resistance increases by $\sim$33% (fig. 5(b)). As the frequency is increased, the air in the perforations oscillates more vigorously, implying that the inertia effect protecting the velocity from changing (relative acoustic mass) decreases. However, in sharp contrast, the existence of roughness enlarges the resistance to velocity changing, leading to a larger acoustic mass.

According to eq. (5), the relative acoustic mass is closely related to the resonant frequency. As shown in fig. 6(a), the resonant frequency decreases significantly with increasing relative roughness and wave number. According to eq. (4), the absorption coefficient depends upon the relative acoustic resistance, peaking when $r = 1$. As surface roughness enhances viscous dissipation, the absorption coefficient of the MPP-R is larger than that of the MPP-S, when all other geometrical and physical parameters remain unchanged. The results of fig. 6(b) reveal further that increasing the relative roughness and/or wave number increases significantly the peak absorption coefficient. Nonetheless, it should be pointed out that, in the extreme case when the relative acoustic resistance of the MPP-S is sufficiently large to ensure $r = 1$, surface roughness may decrease the absorption coefficient of the system.

To better illustrate the influence of surface roughness on the sound absorption coefficient, fig. 7 presents two nephograms, one for the relative roughness and the other for the wave number. The sound absorption coefficient is depicted using different colors, ranging from light to dark as it increases in magnitude. The results of fig. 7 show that, with increasing roughness, the resonant peak is gradually shifted from the lower right to the upper left. That is, in accordance with the variation trends shown in fig. 6, a larger relative roughness and larger wave number can both decrease the resonant frequency and increase the absorption performance of the MPP system.

In conclusion, the classical Maa theory has been successfully modified to account for the effect of surface roughness on sound absorption of microperforated panels (MPPs). Full numerical simulations with the method of finite elements are performed to validate the modified theory and good agreement is achieved. It is demonstrated that the presence of surface roughness decreases the resonant frequency and increases the peak absorption coefficient of the MPP. The remarkable improvement of low-frequency absorption with surface roughness enables designing MPP sound absorbing systems for targeted noise control applications.

* * *

This work was supported by NSFC (11761131003, U1737107 and 11772248), DFG (ZH15/32-1) and the Fundamental Research Funds for the Central Universities (Z201811253).

REFERENCES

[1] Allard J. and Atalla N., *Propagation of Sound in Porous Media: Modelling Sound Absorbing Materials* (John Wiley & Sons, United Kingdom) 2009.
[2] Overvelde J. T., Shan S. and Bertoldi K., *Adv. Mater.*, **24** (2012) 2337.
[3] Ren S., Liu X., Gong J., Tang Y., Xin F., Huang L. and Lu T. J., *EPL*, **120** (2018) 44001.
[4] Maa D. Y., *Sci. Sin.*, **18** (1975) 55.
[5] Maa D. Y., *J. Acoust. Soc. Am.*, **104** (1998) 2861.
[6] García-Chocano V. M., Cabrera S. and Sánchez-Dehesa J., *Appl. Phys. Lett.*, **101** (2012) 184101.
[7] Taylor J. B., Carrano A. L. and Kandlikar S. G., *Int. J. Thermal Sci.*, **45** (2006) 962.
[8] Nikuradse J., *Laws of Flow in Rough Pipes* (National Advisory Committee for Aeronautics, Washington) 1950.
[9] Song S., Yang X., Xin F. and Lu T. J., *Phys. Fluids*, **30** (2018) 023604.
[10] Pride S. R., Morgan F. D. and Gangi A. F., *Phys. Rev. B*, **47** (1993) 4964.